KLOE Note N. 155
9 February 1996

RESULTS FROM A CLUSTER COUNTING MEASUREMENT IN HELIUM-HYDROCARBON MIXTURES

G. Cataldi, F. Grancagnolo and S. Spagnolo

Sezione INFN e Dipartimento di Fisica dell'Università di Lecce, Italy

Abstract

Measurements of primary ionization in mixtures of helium/isobutane and helium/methane have been performed with beams of pions and muons, in the $200 - 300\ MeV/c$ range, impinging on a test drift tube. Preliminary results on the dependence of the number of primary ionization clusters from the gas composition, the particle type and its momentum are illustrated. Extrapolation to a large number of samplings shows that cluster counting provides better particle separation than the traditional technique of truncated mean of dE/dx distributions.

1 Introduction

Gas tracking devices, like drift or proportional chambers, can be used also to provide a measurement of the energy loss along the trajectory of charged particles. The large and inherent uncertenties in total energy deposition, described by Landau-like distribution functions, represent, however, a serious limit to the particle identification capabilities. The large variety of secondary processes contributing to the total energy deposition impairs the good statistical properties of the underlying process: the primary ionization, which is clearly poissonian in nature. A method capable of retrieving this fundamental feature from the produced analog signals could recover the good properties of the primary ionization statistics and allow for a more powerful particle identification.

The cluster counting method [1][2] consists in singling out, in every recorded detector signal, the isolated structures related to the arrival on the anode wire of the electrons belonging to a single ionization act. In order to achieve this goal, special experimental conditions must be met: pulses from electrons belonging to different clusters must have a little chance of overlapping in time and the time interval between pulses generated by electrons coming from the same cluster must be small enough to prevent overcounting. The optimal counting condition can be reached only as a result of the balance between the fluctuations of the processes which prevent a full cluster detection efficiency and of those which enhance the time separation between different ionization events.

A favourable ratio between the mean free path of the ionizing particle and the one of the more energetic primary electrons is a requirement that cannot be disregarded. Therefore small specific ionization is needed in order to have a good localization of each cluster along the track and low diffusion to guarantee a limited swelling up of the cluster along the drift path. Gas mixtures based on helium (4.8 clusters/cm and $\sigma_{diffusion} \sim 200\ \mu m$ for $E/p \geq 800\ Volt/cm\ atm$ [3]) are well suited to cluster counting measurements.

2 Experimental setup

The results presented in this paper come from the analysis of data collected during a test performed at the P.S.I of Villigen (Zurich, Switzerland). The beam consisted of muons and pions with momenta ranging from 150 to 300 MeV/c. A drift tube of square cross section, 2.6 cm side and 2 m length has been used for the primary ionization measurement. The aluminum walls of the detector are 400 μm thick in order to limit the multiple scattering contribution to the measurement of the impact parameter of the beam track to the wire. The sense wire is made of gold plated tungsten with a diameter of 25 μm.

Two MWPC, on each side of the drift tube, allow for a measurement of the impact parameter with an extrapolated error of 200 μm. They are made of four independent planes, x, y, u and v, with u and v rotated by $\pm\pi/6$ with respect

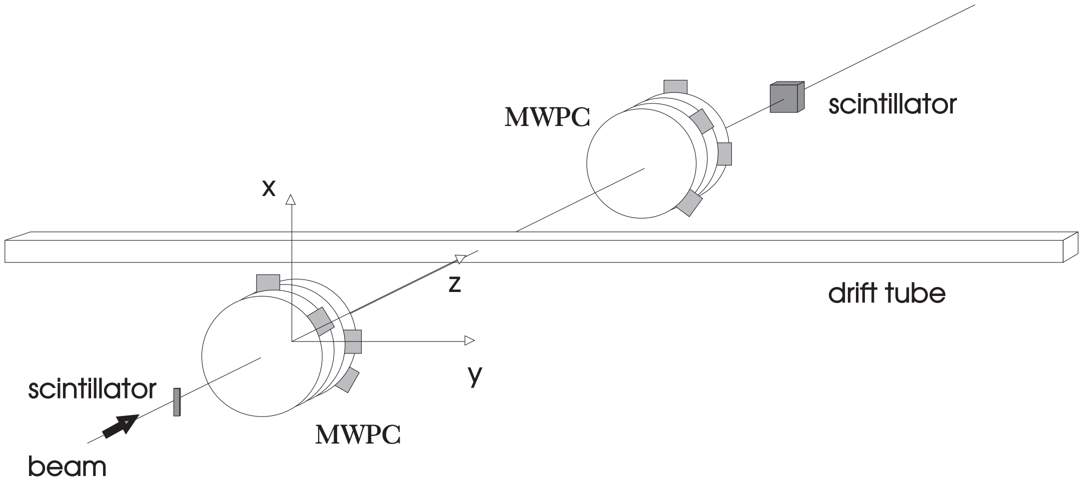

Figure 1: *Layout of cluster counting apparatus.*

to the y plane, with spacing between sense wires of 2 mm. Two scintillators, upstream and downstream of the setup are used for the trigger definition and the measurement of the time of flight, which gives an effective tagging of the pions and the muons occurring in the beam (see fig. 1).

The drift tube wire is connected to a fast (160 ps), wide band (100 KHz to 1.7 GHz) preamplifier (Phillips mod. 6954) in order to preserve substructures with typical times of less than 1 ns. The acquisition of the waveform is performed by a digital sampling oscilloscope (Tektronix mod. 602A), equipped with a circular memory, consisting of three $8 Kbytes$ buffers, bandwidth of 1.1 GHz, 8 $bits$ ADC per channel and sampling rate of 2 Gs/s. All these features allow to record the amplitude of a signal, 4 μs long, every 500 ps.

The acquisition program directs the oscilloscope's operations through the standard IEEE488, and accesses the CAMAC registers where TDCs, ADCs and latches units, dedicated to the drift tube and to all other devices in the experimental setup, reside. The overall size of an event is about 8.7 $Kbytes$. At the end of the run, the acquisition program transfers the data file, in a spawn process, to a Vax station (Digital 4000/60) in order to make it available for monitoring, preanalysis and backup on tape. Details of the experimental setup are given in [4] and [5].

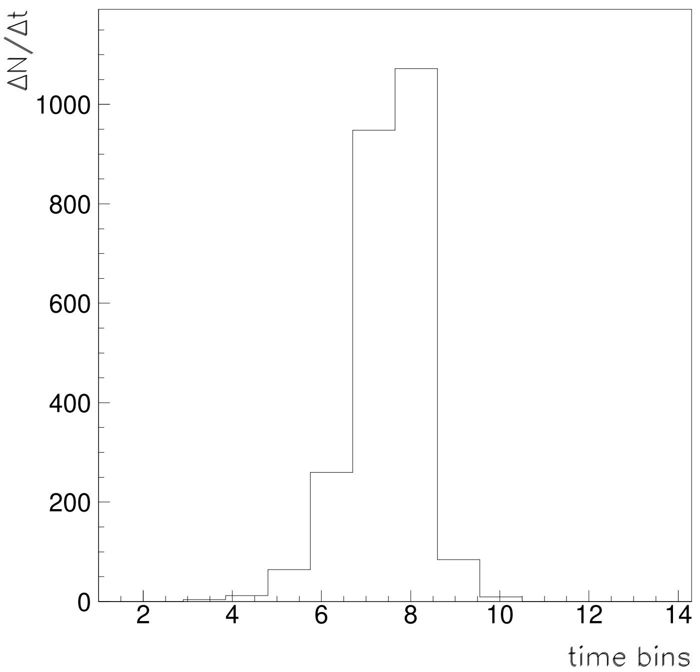

Figure 2: *Distribution of the residues between the arrival time generated in the Monte Carlo and the time at which the search algorithm identifies a cluster. The mean value of the distribution is 7.5 bins, which corresponds to* 3.75 *ns (to be compared with the rise time of the pulse shape generated,* $T_r =$ 3.4 *ns. The root mean square,* 0.4 *ns, is compatible with the digitizer resolution.*

3 Counting algorithm

The algorithm for the off-line counting of the primary cluster consists of a selective search method of local maxima in the array Y(i), which represents the amplitude of the signal in the detector at the time T_i elapsed since the trigger occurrence ($i = T_i \times f_s$, where f_s is the digitizer sampling frequency). In order to reduce the misleading effects of the random white noise and of the long pulse tail, a filtering procedure, based on a smoothing technique, is applied to the local average of the amplitude of the signal.

The local maxima on the smoothed array are identified by looking at the change of the first derivative of the array Y and by checking its consistency with the expected rise and fall times T_r and T_f of the cluster signals. A further selection, based on an amplitude analysis, singles out the recognized clusters from the set of maxima. This is done according to the difference in amplitude between the selected maximum and its adjacent minima and by applying different threshold cuts, depending on the value of the amplitude at the maximum and on its distance from other recognized clusters.

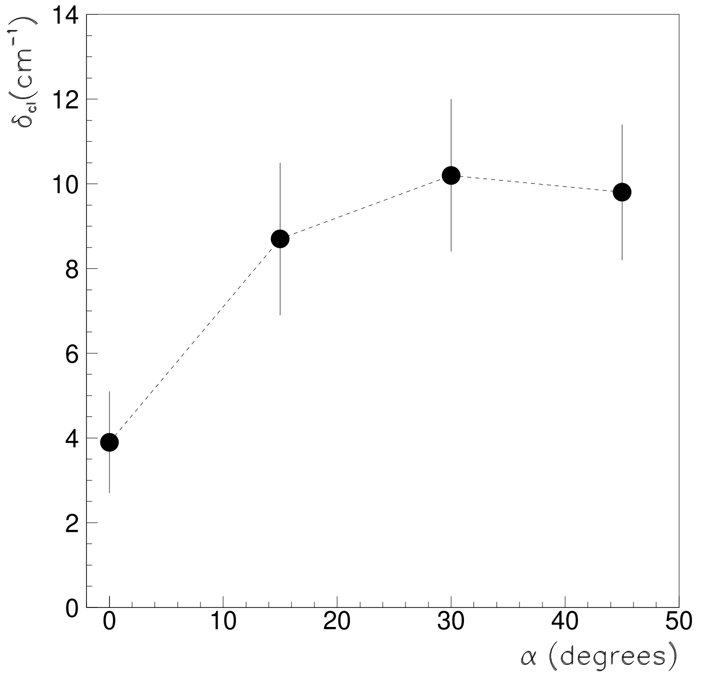

Figure 3: *Clusters density, δ_{cl}, as a function of the angle α between the track and the normal to the tube. The gas mixture used is $95\% He - 5\% i\ C_4H_{10}$ and the beam momentum is 200 MeV/c.*

The efficiency and the reliability of the algorithm have been verified on detailed Monte Carlo simulations of electron drifting in a cell similar to the tube used (see fig. 2) for different gas mixtures (i.e. different drift velocities, diffusion coefficients, primary and secondary ionization). More details are given in [4].

4 Space charge effect

The number of electrons per unit length counted as a function of the angle α, between the track and the normal to the tube wall is shown in fig. 3 for the $95\% He - 5\% i\ C_4H_{10}$ gas mixture. The errors on the measurement are assumed equal to one standard deviation of the relative distributions. The space charge effect is clearly visible. Assuming a cluster density $\delta_{cl} \simeq 10.0\ cluster/cm$ and full counting efficiency for angles larger than 30^o, the typical dimension of the space charge region turns out to be less than 500 μm. Even though the effect is relevant only for angles smaller than 30^o, in the following analysis we refer to data collected with $\alpha = 45^o$ angle.

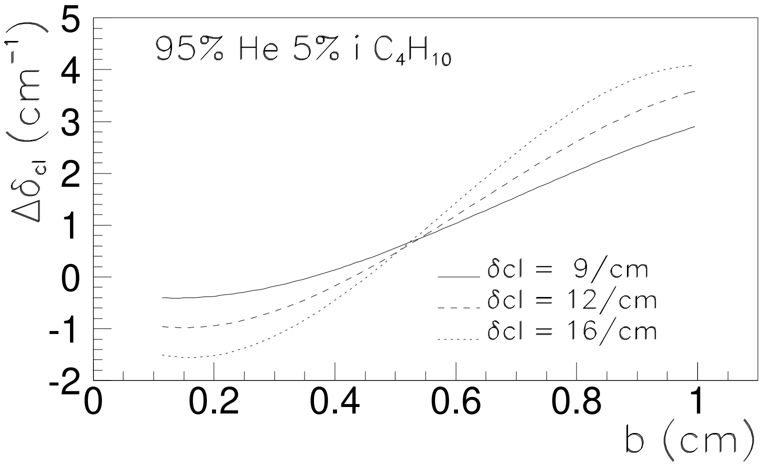

Figure 4: *Differences between the measured cluster density, obtained by applying the counting algorithm to Monte Carlo signals, and the generated one as a function of the impact parameter for* $95\% He - 5\% iC_4H_{10}$. *Analogous differences hold for different gas mixtures. The resolving time here is only due to the counting algorithm* ($\simeq 2.5$ *ns) having digitized the electron signal at* 2 *Gs/s.*

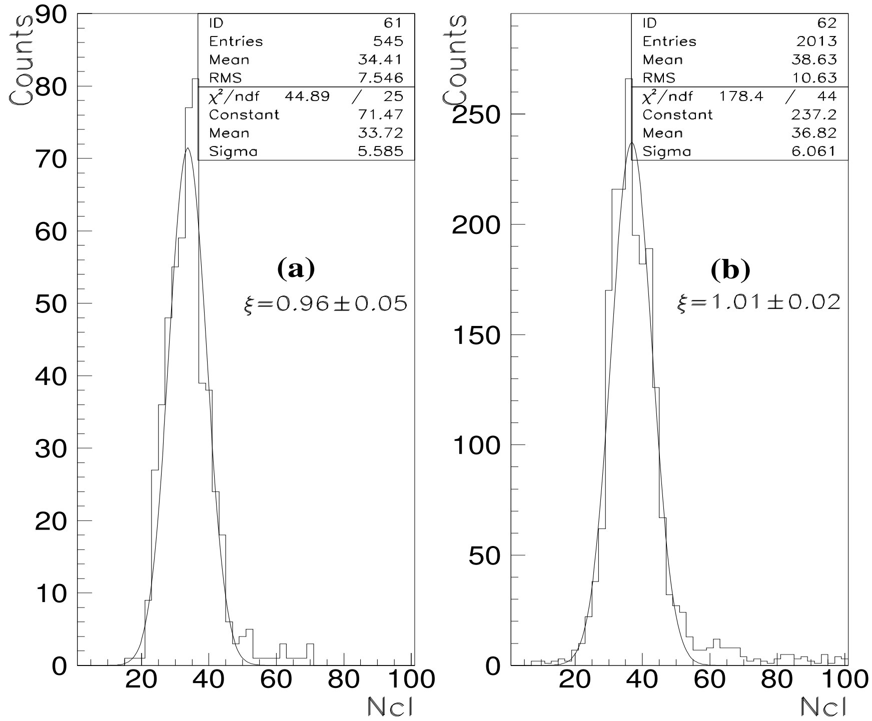

Figure 5: *Distribution of the number of clusters after an iterative application of the correction factor. The pion beam has a momentum of* $280 MeV/c$. *Two different mixtures are shown: (a)* $80\% He - 20\% CH_4$ *and (b)* $95\% He - 5\% i\ C_4H_{10}$.

5 Cluster distributions

As pointed out before, the distribution of the number of clusters produced and counted within a gas sample, a priori Poissonian, is broadened by the dissociation of multi-electron clusters. On the other hand, the overlap of consecutive clusters results in narrowing down such distribution. As a consequence, there might exist conditions − relative to the gas mixture, which affects drift velocity, diffusion and cluster density, to the resolving time, which is determined by the digitizing process and by the counting algorithm, to the impact parameter, to the track length − according to which, some of these effects compensate each other and the resulting distribution of the number of clusters is poissonian and characterized by $\xi = 1$ (ξ is defined as the ratio between the variance of the distribution and the variance of the corresponding poissonian distribution).

The effective counting of primary ionization can therefore be achieved only for a particular set of values of the relevant parameters.

Geometrical effects, which produce undercounting or overcounting depending on the impact parameter (see fig. 4), can be easily corrected with the help of a Monte Carlo (an extensive discussion can be found in [4]). Two examples of counting distributions after an iterative application of correction factors are shown in fig. 5. The superimposed gaussian fit shows how close the distribution is to a poissonian for a fraction of events larger than 95 %. The results obtained for different mixtures and different pion momenta are summarized in Table 1.

Mixture	p_{beam} MeV/c	N_{cl} $(before)$	ξ $(before)$	N_{cl} $(after)$	ξ $(after)$	P_{ee} %
$80\% He$	280	34.4 ± 6.9	1.18 ± 0.06	33.7 ± 5.6	0.96 ± 0.05	3.3
$20\% CH_4$	400	34.2 ± 6.8	1.16 ± 0.07	33.0 ± 5.7	0.99 ± 0.06	4.4
$95\% He$	200	38.9 ± 9.4	1.51 ± 0.06	37.8 ± 6.4	1.04 ± 0.06	4.9
$5\% iC_4H_{10}$	280	38.8 ± 9.3	1.49 ± 0.03	36.8 ± 6.1	1.01 ± 0.02	5.0
$90\% He$	150	70.8 ± 10.0	1.19 ± 0.07	62.3 ± 8.0	1.01 ± 0.05	5.2
$10\% iC_4H_{10}$	200	49.6 ± 9.4	1.33 ± 0.08	46.8 ± 6.9	1.01 ± 0.06	4.1
	270	46.8 ± 9.5	1.39 ± 0.08	45.7 ± 7.0	1.04 ± 0.06	4.8
$85\% He$	250	57.6 ± 8.2	1.08 ± 0.05	56.6 ± 7.4	0.98 ± 0.04	3.8
$15\% iC_4H_{10}$						

Table 1: *Number of clusters before and after the application of corrective factors, P_{ee} is the percentage of events contained in the tail of the distribution after the correction*

6 π/μ separation

Pions and muons in the beam can be tagged by the time of flight between the trigger scintillators (see fig. 6). In order to compare the cluster counting and dE/dx performances as far as particle identification is concerned, different sets

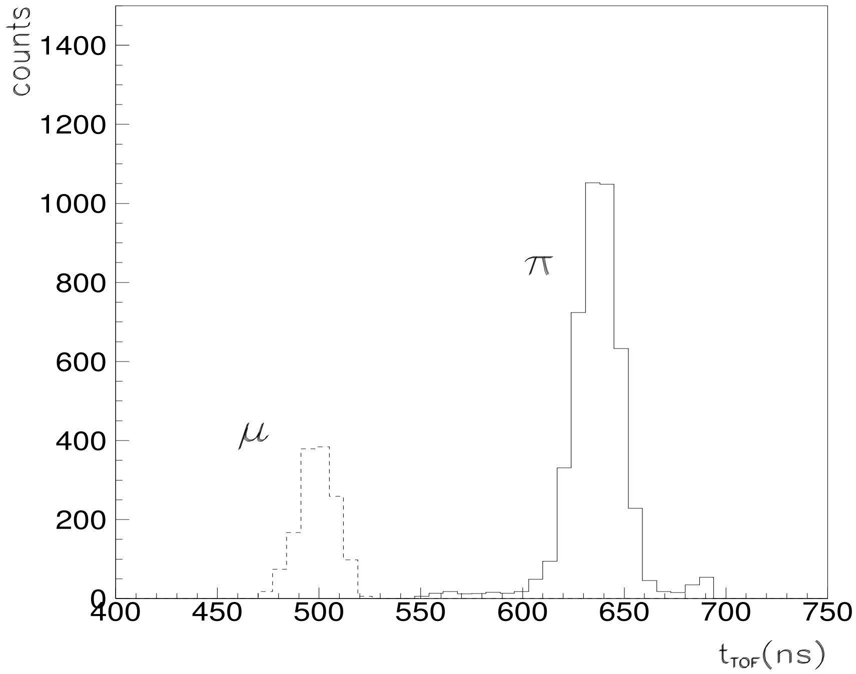

Figure 6: *Time of flight for a* $200 MeV/c$ *beam.*

of measurements corresponding to different track lengths have been simulated by adding up events extracted according to the cluster (or dE/dx) distributions in a single cell for the two particle types. The set of data used refers to the $95\% He - 5\% iC_4H_{10}$ gas mixture and to beam momenta of 200 and 280 MeV/c.

The dE/dx measurement is obtained by a numerical integration of the digitized signal. Fig. 7 shows the dE/dx distributions for π and μ from a single cell measurement and for the sum of 100 measurements extracted from such distributions to simulate long tracks. The sampling length is about 3.7 cm. The long high energy deposition tails in the single cell distributions come from the typical Landau-like behaviour of the dE/dx measurement. Fig. 8 represents the dE/dx resolution, as a function of the number of samples on the track. With the traditional technique of the truncated mean, the best π/μ separation is achieved by cutting away 20% of the highest energy depositions along the track (fig. 9) independently of the total number of samplings. In this conditions the optimal separation increases according to the square root of the number of samples as in fig. 10.

Analogously, from the same data, cluster distributions for single cell and 100 times sampled tracks are shown in fig. 11, while the resolution as a function of the sampling is reported in fig. 12. The π/μ separation provided by the cluster counting technique is compared in fig. 13 with the separation obtained with the 20% truncated mean algorithm. Fig. 13 shows also the best π/μ discrimination

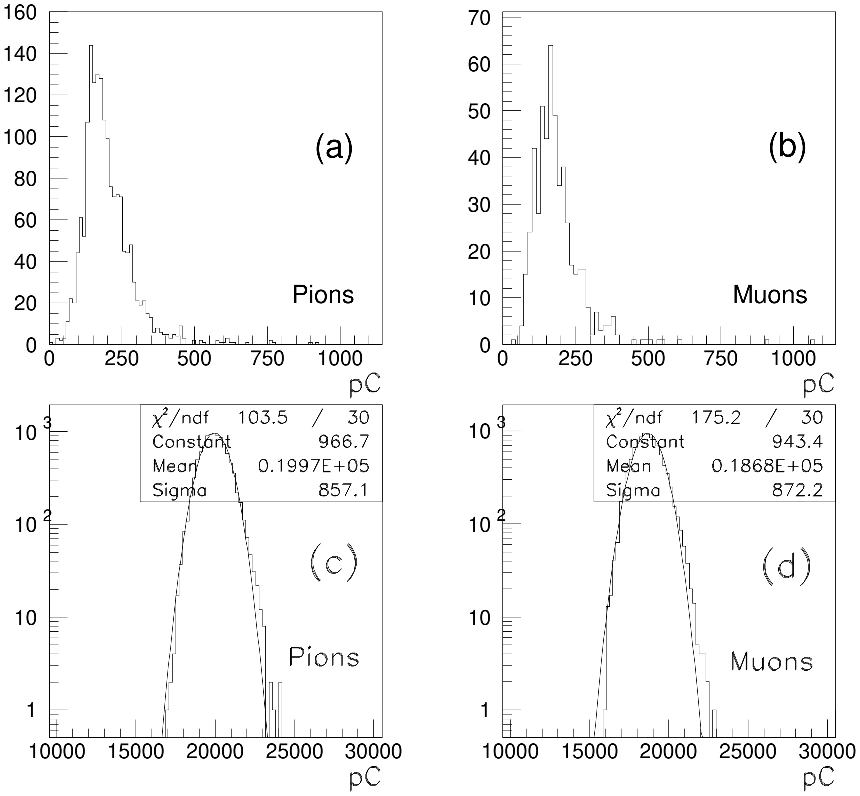

Figure 7: *Distributions of the collected charge, which is proportionally related to the dE/dx, from single cell measurements ((a) pions, (b) muons) and for the sum of* 100 *measurements extracted from such distributions to simulate a long track ((c) pions, (d) muons). Sample length is about* 3.7 *cm. Data refer to* $200 MeV/c$ *beam momentum and* $95\% He - 5\% iC_4H_{10}$ *gas mixture.*

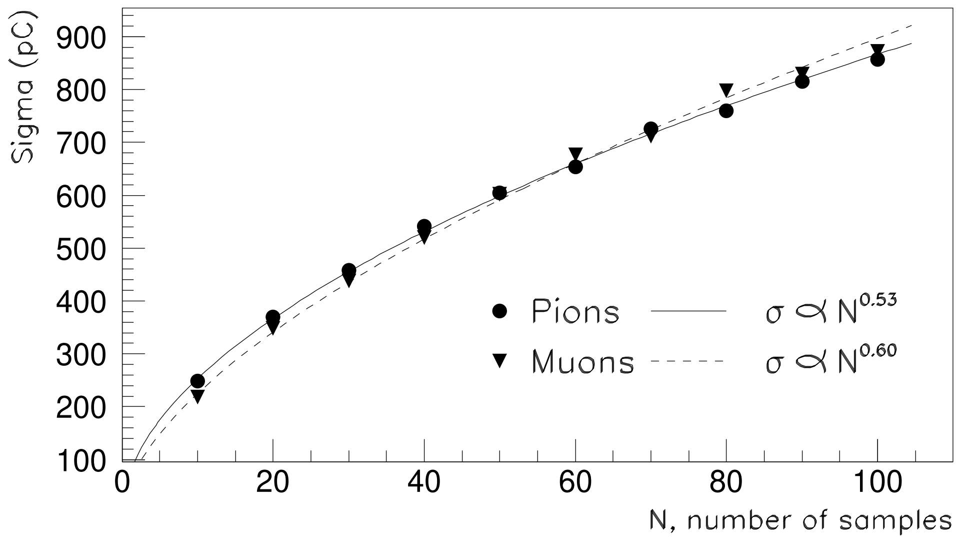

Figure 8: *dE/dx resolution as a function of the number of samplings along the track. Sample length is about* 3.7 *cm.*

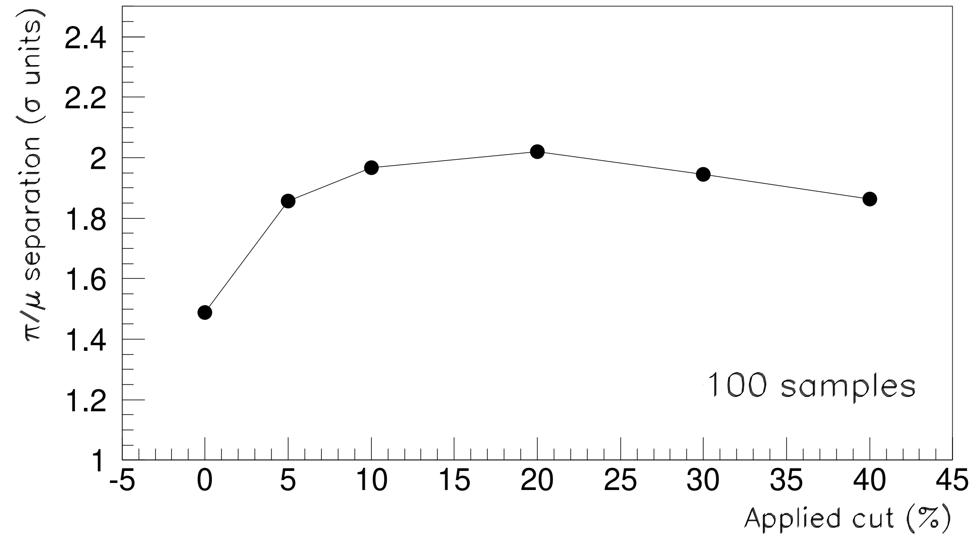

Figure 9: *π/μ average separation of a dE/dx measurement over* 100 *samples as a function of the rejected hit percentage with the largest values.*

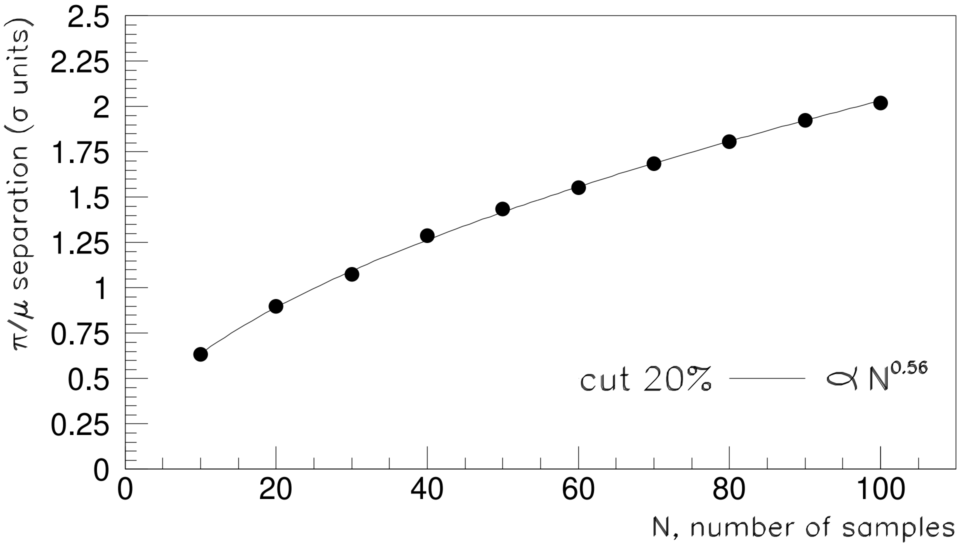

Figure 10: *Optimal π/μ separation from a dE/dx measurement as a function of the track sampling. The rejected hit percentage is* 20%.

achievable by an ideal cluster counting measurement. This has been evaluated by extracting the single cell measurements not from the experimental cluster distribution but from a gaussian fit to it.

The available data sample unfortunately allows us to study the π/μ separation only for two values of the particles momenta: 200 and 280 MeV/c. The overall results for 100 times sampled tracks, sample length 3.7 cm, in $95\%He-5\%iC_4H_{10}$ are plotted in fig. 14 together with theoretical evaluations of the dE/dx resolution with the usual parametrization [2]:

$$\sigma(\%) = 40.7n^{-0.43}l^{-0.32} \tag{1}$$

where n is the total number of samples and l is the sampling length.

7 The dE/dx and the dN/dx curves

The total ionization, produced in a gas mixture, is correlated to the specific energy loss by the average energy w required for the production of one electron-ion pair. Neglecting non linear effects, it is possible to consider the total ionization as given by:

$$\left(\frac{dN}{dx}\right)_t = \frac{p_1}{w_1}\left(\frac{dE}{dx}\right)_1 + \frac{p_2}{w_2}\left(\frac{dE}{dx}\right)_2 \tag{2}$$

where p_1 and p_2 are the helium and the hydrocarbon percentages. Analogously, assuming that $< N_e >$ is the mean electron population in each cluster, we can write for the primary ionization:

$$\left(\frac{dN}{dx}\right)_p = \frac{1}{< N_e >_1}\frac{p_1}{w_1}\left(\frac{dE}{dx}\right)_1 + \frac{1}{< N_e >_2}\frac{p_2}{w_2}\left(\frac{dE}{dx}\right)_2 \tag{3}$$

The dE/dx curves, inferred by the Bethe-Bloch parametrization, are superimposed in fig. 15 to the experimental data. The agreement is reasonably good, given the errors. It is possible to determine the cluster density more accurately by taking into account the distribution of clusters for the long tracks as defined in the previous paragraph, for $200MeV/c$ and $280MeV/c$ momentum pions in $95\%He - 5\%iC_4H_{10}$ gas mixture:

$$\delta_{cl,200} = 10.10 \pm 0.50\ clusters/cm \tag{4}$$

$$\delta_{cl,280} = 9.65 \pm 0.47\ clusters/cm \tag{5}$$

Expressing equation (3) as:

$$\frac{dN}{dx} = \delta_{cl} = K_1p_1\left(\frac{dE}{dx}\right)_1 + K_2p_2\left(\frac{dE}{dx}\right)_2 \tag{6}$$

we can fit the best values of the constants K_1 and K_2 obtaining, for minimum ionizing pions:

$$\delta_{cl,He} = 5.5 \pm 0.9\ clusters/cm \tag{7}$$

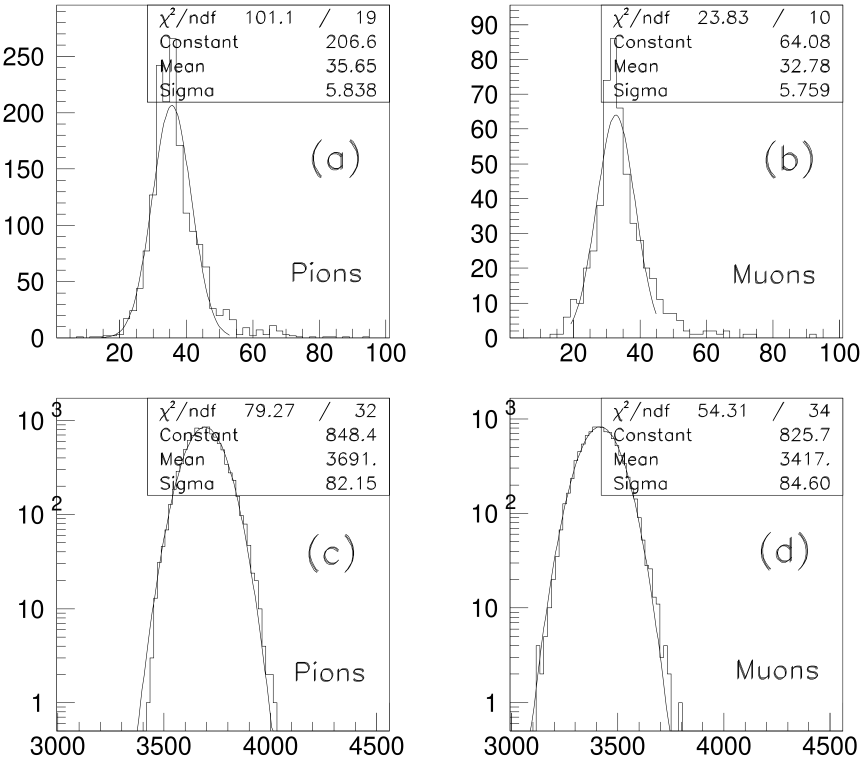

Figure 11: *Cluster distributions from single cell measurements ((a) pions, (b) muons) and for* 100 *cells sampling a track ((c) pions, (d) muons). Data refer to* $200 MeV/c$ *beam momentum and* $95\% He - 5\% iC_4H_{10}$ *gas mixture.*

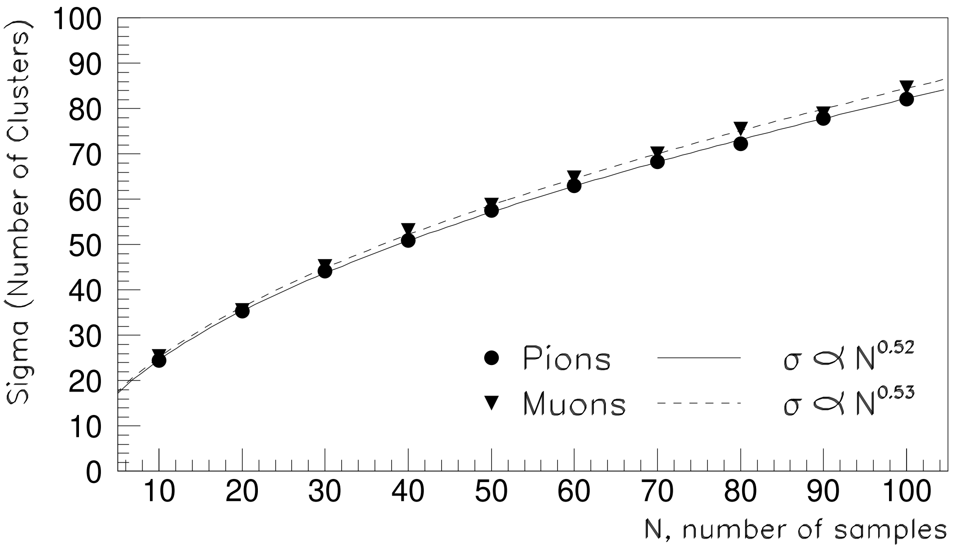

Figure 12: *Cluster counting resolution as a function of the track sampling.*

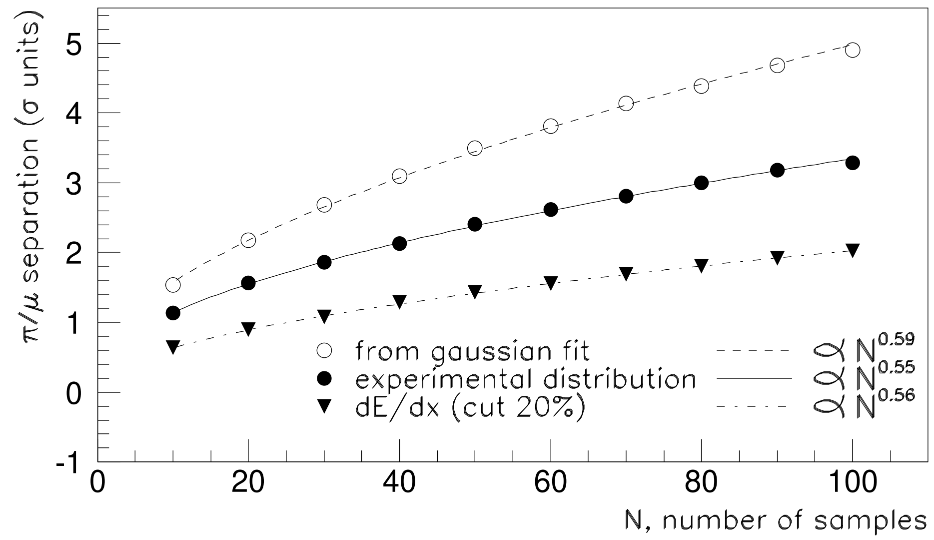

Figure 13: *π/μ separation from a cluster counting measurement as a function of the track sampling. For comparison the optimized dE/dx result and the ideal cluster counting separation are superimposed.*

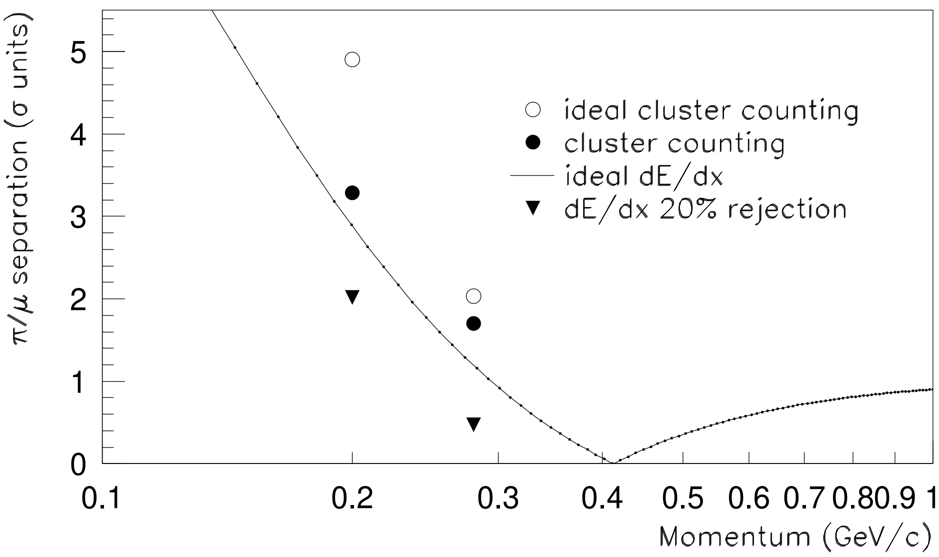

Figure 14: *π/μ separation as a function of the particle momentum. The solid line is an empirical extrapolation from existing data.*

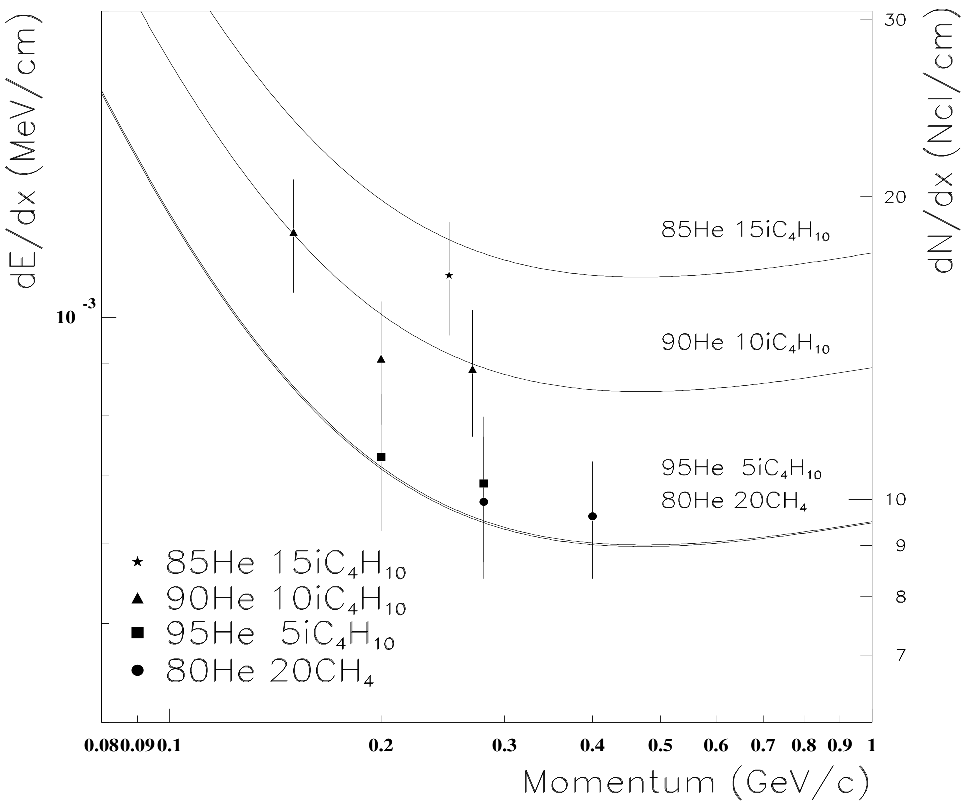

Figure 15: *Bethe-Bloch parametrization of dE/dx for pions, superimposed to the experimental data.*

$$\delta_{cl,iC_4H_{10}} = 70 \pm 12 \; clusters/cm \tag{8}$$

These values are in good agreement with ref. [3].

8 Conclusions

The cluster counting technique described shows that this method could be successfully applied to a conventional cell in a standard drift chamber, provided that a helium based gas mixture is used, thanks its low primary ionization ($\simeq 5 \; clusters/cm$) and low drift velocity ($1-2 \; cm/\mu s$), and that the signal is digitized at sampling rates of the order of $1-2 \; Gs/s$. Obviously, the difficult task of handling enormous amount of data, which is of great concern in designing a large scale detector, is here ignored.

Despite of a largely incomplete set of experimental data, this analysis shows that rejection factors for π/μ separation from two to four times larger than the corresponding dE/dx traditional measurement (truncated mean) can be obtained for track lengths of the order of $3 - 4$ m in the range of momentum of $200 - 300$ MeV/c.

It is worth mentioning that the precision of this measurement, which follows a Poisson distribution, unlike the case of Landau distributions, will further improve with the track length.

Acknowledgements

We thank the KLOE collaboration which encouraged us to proceed towards a feasibility study of the cluster counting method. In particular, we tank L. Cerrito, M. Imhof, L. Paoluzi and S. Weseler for the useful and stimulating discussions which led to the test and for their effortless presence during the data taking phase. We also thank P. Creti and M. Panareo for setting up a very efficient data acquisition system and G. Fiore, R. Gerardi and C. Pinto for the technical support before and during the test.

References

[1] V. A. Davidenko *et al*, NIM **67** (1969) 325-330
V. A. Chechin *et al*, NIM **98** (1972) 577
A. H. Walenta, IEEE, vol.NS-26, n^0 1 (1979)
F. Lapique and F. Piuz, NIM **175** (1980) 297-318
J. H. Cobb, W. W. M. Allison e J. N. Bunch, NIM **133** (1976) 315-323
A. Breskin *et al*, NIM **A252** (1986) 488-497
A. Breskin *et al*, IEEE, vol.36, n^0 1 (1989)
G. Malamud *et al*, NIM **A307** (1991) 83-96
A. Pansky *et al*, NIM **A323** (1992) 294-308

[2] A. H. Walenta, IEEE, vol.NS-26, n^0 1 (1979)

[3] A. Sharma and F. Sauli, CERN-PPE/93-51 10 Febbraio 1993

[4] G. Cataldi, 'Il problema della separazione π/μ nella camera a $drift$ di KLOE', tesi di dottorato, Feb. 1995, Consortium of Universities of Bari and Lecce, *unpublished*

[5] S. Spagnolo, 'La camera a drift di KLOE: definizione dei parametri e misure di ionizzazione primaria in miscele di elio', tesi di laurea, Dec. 1993, University of Lecce, *unpublished*